Unveiling ecological assembly rules from commonalities in trait distributions

Nicolas Gross, Yoann Le Bagousse-Pinguet, Pierre Liancourt, Hugo Saiz, Cyrille Violle, François Munoz

ECOLOGY LETTERS

Unveiling ecological assembly rules from trait distributions

Journal:	*Ecology Letters*
Manuscript ID	ELE-01217-2020.R1
Manuscript Type:	Letters
Date Submitted by the Author:	14-Feb-2021
Complete List of Authors:	Gross, Nicolas; INRAE, ECODIV Pinguet, Yoann Liancourt, Pierre; Czech Academy of Sciences, institute of botany; University of Tubingen Faculty of Science, Plant Ecology Group Saiz, Hugo Violle, Cyrille; CNRS, CEFE Munoz, François; Université Grenoble Alpes, Laboratoire d'Ecologie Alpine

Letters

Running head Trait diversity and assembly rules

Title: Unveiling ecological assembly rules from trait distributions

Nicolas Gross[1,†,*], Yoann Le Bagousse-Pinguet[2,*], Pierre Liancourt[3,4,*], Hugo Saiz[5], Cyrille Violle[6], François Munoz[7]

[1] Université Clermont Auvergne, INRAE, VetAgro Sup, UMR Ecosystème Prairial, 63000 Clermont-Ferrand, France.

[2] Aix Marseille Univ, CNRS, Avignon Université, IRD, IMBE, Technopôle Arbois-Méditerranée Bât. Villemin – BP 80, F-13545 Aix-en-Provence cedex 04, France.

[3] Institute of Botany of the Czech Academy of Science, Průhonice, Czech Republic

[4] Plant Ecology Group, University of Tübingen, Tübingen, Germany

[5] Institute of Plant Sciences, University of Bern. Altenbergrain 21, 3013 Bern, Switzerland.

[6] Centre d'Écologie Fonctionnelle et Évolutive UMR 5175, Univ Montpellier – CNRS – EPHE - IRD –Univ Paul Valéry Montpellier, 1919 route de Mende, 34293 Montpellier Cedex 5, France

[7] Univ. Grenoble Alpes, LIPHY, F-38000 Grenoble, France

† Corresponding Author: nicolas.gross@inrae.fr

*these authors can be considered as co-first authors

Author contributions

NG, YLB-P. and PL developed the original idea. FM developed the model and the coding. NG ran the simulations. All co-authors contributed to data interpretation. NG and YLB-P wrote the first draft of the paper with major contribution from all co-authors.

Data accessibility statement: This paper is based on simulations. The authors provide the R code to generate the simulations with the submitted manuscript. The R code will be archived in an appropriate public repository with the acceptance of the paper.

Word count:

Abstract: 149 words

Main Text: 4566 words

Box 1: 657 words

Number of references: 50

Number of Figures: 5

Number of Box: 1 text box

ABSTRACT

Deciphering the effect of neutral and deterministic processes on community assembly is critical to understand and predict diversity patterns. The information held in community trait distributions is commonly assumed as a signature of these processes, but empirical and modelling attempts have most often failed to untangle their confounding, sometimes opposing, impacts. Here, we simulated the assembly of trait distributions through stochastic (dispersal limitation) and/or deterministic scenarios (environmental filtering, niche differentiation). We characterized the shape of trait distributions through the skewness-kurtosis relationship. We identified commonalities in the co-variation between the skewness and the kurtosis of trait distributions with a unique signature for each simulated assembly scenario. Our findings were robust to variation in the composition of regional species pools, dispersal limitation, and environmental conditions. While ecological communities can exhibit a high degree of idiosyncrasy, identification of commonalities across multiple communities can help to unveil ecological assembly rules in real-world ecosystems.

Key words: dispersal limitation, community assembly rules, environmental filtering, functional diversity, niche differentiation, skewness-kurtosis relationship, stochasticity, trait distributions

INTRODUCTION

A basic tenet in community ecology is that trait diversity can reveal the influence of deterministic processes on species assemblages (e.g., competition and abiotic factors; McGill *et al.* 2006; Weiher *et al.* 2011). Central to this research agenda is the hypothesis that high trait diversity reflects niche differentiation processes, while low trait diversity reflects the effect of environmental filtering selecting for species with similar trait values (Cornwell & Ackerly 2009; Maire *et al.* 2012; Keddy 1992; Grime 2006). Much research has been devoted to analyze how patterns of trait diversity vary within and among communities (e.g., convergence or divergence) with the aim to uncover general assembly rules that could apply across many ecosystems (Diamond 1975; Weiher & Keddy 2001). However, hypothesizing a direct and unequivocal linkage between patterns of trait diversity and assembly processes has proved too simplistic and fed much debate (Weiher *et al.* 2011; Götzenberger *et al.* 2012; Münkemüller *et al.* 2020).

Multiple assembly processes are likely to simultaneously influence local trait diversity, sometimes in opposite directions (Mayfield & Levine 2010; Maire *et al.* 2012), making trait diversity patterns often difficult to distinguish from randomness (Götzenberger *et al.* 2012; Munoz & Huneman 2016). The signature of deterministic processes can be blurred by stochastic processes such as demographic drift, or contingent variation in the regional species pool composition (Hubbell 2001; Spasojevic *et al.* 2018). Furthermore, most trait-based approaches have ignored the effect of species dispersal among communities (Spasojevic *et al.* 2014). Dispersal limitation can strongly reduce species richness (Ricklefs 1987), increasing the imprint of local demographic stochasticity (Leibold *et al.* 2004), and thereby yielding apparent randomness in community-level patterns (Götzenberger *et al.* 2012; Munoz & Huneman 2016). Deciphering how multiple stochastic and deterministic processes shape trait diversity is not only crucial to expand our fundamental understanding of biodiversity patterns, but also to better predict the response of communities and ecosystems to ongoing environmental changes.

Trait diversity is usually assessed using synthetic indices derived from the distribution of trait values within communities (e.g., Mason *et al.* 2005; Laliberté & Legendre 2010; Enquist *et al.* 2015; Carmona *et al.* 2016). Most studies focus on the mean and variance/dispersion of trait distributions (Violle *et al.* 2012), or on related indices (e.g., FDis, Laliberté & Legendre 2010). Considering that mean and variance suffice for describing trait diversity relies on the implicit assumption that trait values follow (approximately) a normal distribution. In essence, the normal distribution shows a bell shape, whose mean represents a local optimum that matches a given environment and the variance represents how trait values are constrained around this mean (Enquist *et al.* 2015, Fig. 1a). However, trait distributions often deviate from a normal distribution in real-world communities, and can exhibit asymmetric, flat, peaky or multimodal shapes (Fig. 1b) (Enquist *et al.* 2017; Le Bagousse-Pinguet *et al.* 2017). In such cases, further information on the shape of trait distributions is required to characterize trait diversity.

The shape of trait distributions can be quantified by the skewness and the kurtosis, which quantify the asymmetry and the evenness of the trait distributions, respectively. The skewness and the kurtosis are increasingly used in ecological research because they can provide insights on how species assemble within communities, and how they respond to ongoing environmental changes (Kraft *et al.* 2008; Enquist *et al.* 2015; Gross *et al.* 2017; Wieczynski *et al.* 2019). For instance, rapid environmental changes can simultaneously increase the skewness and kurtosis of trait distributions when a limited portion of the community with specific trait values benefit from the environmental change, and the recruitment of new species adapted to novel conditions is not immediate (see predictions in "Trait Driver Theory" in Enquist *et al.* 2015, 2017). Conversely, niche differentiation should decrease the kurtosis of trait distributions, yielding flatter or even bimodal distributions by promoting the coexistence of functionally contrasting species (Cornwell & Ackerly 2009; Maire *et al.* 2012) .

The skewness and the kurtosis are mathematically constrained through the Skewness-Kurtosis Relationship (SKR hereafter), which can be used to characterize a broad spectrum of distributions (Box 1) (Cullen & Frey 1999). Across a variety of dryland plant communities, Gross et al. (2017) reported that the distributions of plant height and specific leaf area followed non-random SKRs. These empirical SKRs suggested the existence of general assembly rules observable at the biome scale where traits organized according to specific families of trait distributions (see Box 1 and Fig. 1c;d for a definition of family of trait distributions). Yet, we do not know which ecological processes underpin such empirical assembly rules, how different deterministic and stochastic processes modulate SKR patterns, and whether the signature of these processes are distinguishable from one another. A theoretical evaluation of the SKR framework is therefore needed to assess the effects of multiple stochastic and deterministic assembly processes on trait distributions, and more generally, to advance our ability to identify assembly rules from patterns of trait distributions.

In a theoretical experiment, we simulated the effects of multiple stochastic and deterministic processes on trait diversity patterns. Using the *ecolottery* package in R language (Munoz *et al.* 2018), we generated 800,000 communities spanning a broad spectrum of ecological processes and of resulting trait distributions. Specifically, we considered four community assembly scenarios: (i) a purely neutral scenario including stochastic processes only; and (ii) three different "trait-based" scenarios, each combining stochastic processes with a distinct outcome of deterministic processes entailing either convergence or divergence in trait distributions (Loranger *et al.* 2018). Our goals were:

(1) to assess the extent to which the SKR and standard metrics of trait diversity capture distinguishable signatures of assembly processes;

(2) to evaluate how the importance of stochastic processes (through the manipulation of the regional species pool richness, and dispersal limitation among communities) and

environmental variations across communities affect our ability to identify unambiguous signatures of the four community assembly scenarios.

METHODS

Community assembly scenarios

ecolottery is a modeling platform simulating the assembly of ecological communities (Munoz *et al.* 2018). It relies on a spatially implicit framework in which communities are assembled from an external pool of potential immigrants (e.g., a regional species pool) through dispersal. Stochastic and deterministic processes can be parameterized in *ecolottery*. They both influence the establishment success of immigrants and survival of their descendants in the model (Loranger *et al.* 2018; Munoz *et al.* 2018). Stochastic processes influence local diversity through demographic drift, dispersal limitation, and species richness in the regional pool (Etienne & Alonso 2005). Deterministic processes modulate the success of immigrants based on how their trait values allow establishment and persistence in local environments.

We simulated three different outcomes of deterministic processes in *ecolottery* henceforth "trait-based filtering". The first trait-based filtering operates around a single optimal value defined by its matching with the local environmental conditions ("stabilizing filtering" hereafter), consistently with the classical view of the environmental filtering (Keddy 1992; Kraft *et al.* 2015). Stabilizing filtering typically generates normal or more leptokurtic distributions (e.g. hyperbolic distributions, Fig. 1 a,b), depending on the strength of the filtering (Enquist *et al.* 2015; Le Bagousse-Pinguet *et al.* 2017). The second trait-based filtering generates assemblages where alternative optimal trait values can confer greater species performance ("disruptive filtering"; Rolhauser & Pucheta 2017; Loranger *et al.* 2018). This trait-based filtering produces patterns that reflect either niche differentiation among functionally contrasting species (Cornwell & Ackerly 2009; Maire *et al.* 2012; Rolhauser &

Pucheta 2017). Disruptive filtering typically produces uniform or bimodal distributions (Fig. 1b). Finally, the third trait-based filtering generates assemblages in which species performance varies monotonically with trait values ("Directional filtering"). This produces asymmetric trait distributions (Loranger *et al.* 2018) (e.g. exponential distribution in Fig. 1b), e.g. in the case of asymmetric light competition (Schamp *et al.* 2007) or directional environmental changes (Enquist *et al.* 2015).

In silico assembly experiment

We considered four theoretical scenarios to assemble communities: (i) a purely neutral scenario that only considers the effect of stochastic processes on assembly without influence of trait differences on species performance and on trait distribution in assemblages (Hubbell 2001); and (ii) three contrasting scenarios in which deterministic processes (aforementioned trait-based filtering) are combined with stochastic processes. We modeled the four scenarios using different values of the parameter "*filt*" in *ecolottery* to represent the "neutral", "stabilizing", "disruptive" and "directional" scenarios (see R code in Appendix S1 in Supporting Information). In addition, we draw species trait values *i* between -3 to +3.

In a first simulation experiment, we simulated all communities with the same environmental conditions ("fixed environment", hereafter), under low or high dispersal limitation. Dispersal limitation was manipulated using a migration parameter "*m*" that was set to either low (m = 0.95) or high dispersal limitation (m = 0.05). In a second simulation experiment, we simulated communities along an environmental gradient. The environmental gradient was simulated by adjusting the parameter "*Env*" from -2 to + 2, corresponding to the two extremes of a gradient (e.g., from cold to hot environments), and where 0 represented the mild environment (see Table S1 for model parameters). We chose the range of environmental variation "*Env*" (ranging from -2 to + 2) to be lower than the range of possible trait values

(ranging from -3 to +3) to avoid edge effects (Denelle *et al.* 2019). We set "*m*" to either low or high dispersal limitation as explained in the first simulation experiment.

The total number of individuals in the external species pool was set to 25,000. This pool delineates the 'regional species pool' in our simulations. To evaluate how the richness of the species pool influenced community assembly, the pool of immigrants varied from 10 to 500 species. Richness at the regional level was fixed for each simulation run. The total number of individuals per community was set to 250 (Table S1), and we simulated 100 communities in each run. We chose these parameter values to approximate "realistic" vegetation sampling in the context of dryland (Gross et al. 2017, Table S1). Within communities, the number of individuals per species could vary according to the simulated assembly processes. The trait values of the regional species pool followed a uniform distribution, such that all trait values had equal probability of being selected. We randomly assigned trait values to each species. During this procedure, the model allowed different species to exhibit similar trait values, therefore allowing functional redundancy to occur among species (Munoz *et al.* 2018). For simplicity, we did not consider intraspecific trait variability in our simulations. Conspecific individuals thus displayed the same trait value.

Analysis of simulated trait distributions

We generated 800,000 communities: 500 runs where species richness varied from 10 to 500 species in the species pool × 100 communities per run × 4 scenarios × 2 levels of dispersal limitation (low vs. high) × 2 environmental contexts (a fixed environment vs. an environmental gradient). For each run, we recorded the total number of species in a given community (species richness). We quantified species relative abundance as the relative frequency of each species in each community (i.e., the number of individual of a species divided by the total number of individual in the community).

We calculated the four moments of the trait distribution associated to each simulated community: the mean, variance, skewness and kurtosis. Then, we calculated the parameters of the SKRs across the 100 simulated distributions obtained from each run (R^2, slope, Y-intercept and the distance to the lower boundary; see Box 1). For each community, we also computed classical indices of trait diversity using the dbFD function in the "FD" package in R [functional dispersion (FDis), the Rao index, functional evenness (FEve); Laliberté and Legendre 2010]. The four distribution moments and all trait diversity metrics were abundance-weighted. While the SKR parameters were estimated across the 100 communities generated by each simulation run, the four distribution moments, and taxonomic and trait diversity indices were calculated at the community level, and thus generated 100 values for each run.

We evaluated whether the parameters of the SKRs, the four distribution moments and all diversity metrics can be used to discriminate assembly processes from trait distributions. For instance, lower variance, FDis and Rao values compared to the neutral scenario are expected for the stabilizing and directional filtering, i.e., trait convergence. Conversely, higher variance, FDis and Rao values compared to the neutral scenario are expected for the disruptive filtering, i.e., trait divergence. To test for significant differences among scenarios, we used the "overlap" package in R (Ridout & Linkie 2009). For each diversity metric, we calculated the overlap between each pair of scenarios and the mean overlap considering all scenarios together. Overlap values ranged from 0 to 1. An overlap < 0.05 indicated that the metric under consideration significantly discriminate assembly scenarios.

RESULTS

Discriminating scenarios using functional diversity metrics

The neutral scenario generated a wide range of trait diversity patterns, which challenges the inference of ecological processes from trait distributions (Figs. 2, 3). Significant differences

among scenarios were observed under low dispersal limitation. For instance, we observed significant differences between the stabilizing and the neutral scenarios for FDis and for Rao under low dispersal limitation (Figs. 2, 3). However, under high dispersal limitation, all trait diversity indices - with the exception of the variance - simulated under the neutral scenario systematically overlapped with those of the deterministic scenarios, meaning a lack of differences among them.

The variance of trait distributions best discriminated assembly scenarios. We observed a low mean overlap (Mo) when dispersal limitation was low and under fixed environment (Mo = 0.01, Fig. 2a, left panel). The stabilizing and directional scenarios exhibited significantly lower variances than those of the neutral scenario. However, the variance could not discriminate the stabilizing from the disruptive and directional scenarios, and the neutral from the disruptive scenario along an environmental gradient combined with high dispersal limitation (Mo = 0.16, Fig. 2b). Overall, our results showed limited ability of these metrics of trait diversity to identify unambiguous signatures of the four community assembly scenarios.

SKR parameters simulated in a fixed environment

Each studied scenario generated contrasting SKR patterns under fixed environmental conditions and low dispersal limitation (Fig. 4, see also SKR plots in Fig. S1). The neutral and stabilizing scenarios both generated weaker SKRs than the disruptive and directional scenarios (significantly lower R^2, Fig. 4b). These first two scenarios produced distributions that clustered in the skewness-kurtosis space, and tended to overall converge toward a single skewness-kurtosis coordinate as species richness in the regional pool increased (from dark to bright blue dots, Fig. 4a). In contrast, both the directional and the disruptive scenarios yielded strong SKRs, i.e. characterized by significantly higher R^2 than neutral and stabilizing scenarios (Fig. 4b). Specifically, the disruptive scenario generated SKRs with the highest R^2, ranging from 0.6 to

0.99 (Fig. 4b), indicating that all communities assembled under this scenario belong to a unique family of trait distributions (skew-bimodal distribution, Fig. 1c, d).

The SKRs generated from the four scenarios had also clear and significantly distinct Y-intercepts (Fig. 4b). Therefore, the SKR not only discriminated the three scenarios containing deterministic processes from a purely neutral scenario, but also clearly differentiated these three scenarios from one another. The neutral scenario had a Y-intercept = 1.86 (Fig. 4b) suggesting that it converged toward uniform distribution (Fig. 1b). This pattern of trait diversity observed at the Y-intercept of the SKR thus mirrored the trait distribution of the regional pool. The stabilizing scenario produced communities that converged toward a normal distribution (Y-intercept = 2.82 Fig. 4b). This scenario generated a peakier and therefore less even trait distribution than the neutral one. The directional scenario generated distributions that were mostly asymmetric, and that converged toward a skewness value ~1 as species richness increased (Fig. 4a) and a Y-intercept = 2.1 (Fig. 4b). The disruptive scenario had the lowest Y-intercept = 1.33 (Fig. 4b). This scenario generated a family of trait distributions approaching the lower boundary of the skewness-kurtosis space, corresponding to highly platykurtic bimodal distributions (see the skew-bimodal distribution in Fig. 1c). Therefore, the disruptive scenario was the one with the highest trait diversity in our simulations.

Increasing the influence of stochasticity, through high dispersal limitation, reduced the species richness at the community level (Fig. S2). It consistently increased the asymmetry of trait distributions for all scenarios, thereby increasing the scatter of distributions in the skewness-kurtosis space (Fig. 4a). Higher scattering of skewness and kurtosis values produced SKRs with higher R^2 for all scenarios (Fig. 4b). For instance, the R^2 of the neutral scenario ranged from 0.25 to 0.75 (Fig. 4b), indicating that significant SKRs can be observed and produced by a high stochasticity even under a strictly neutral scenario. Yet, irrespective of the degree of stochasticity, the disruptive filtering always produced the strongest SKRs (Fig. 4b).

Furthermore, increasing dispersal limitation marginally influenced the Y-intercept of the SKRs. The mean overlap among scenarios remained extremely low under high dispersal limitation (Y-intercept: Mo = 0.03, Fig. 4b). We observed significant differences between the stabilizing, neutral and disruptive scenarios, although the directional scenario overlapped with the neutral one (overlap = 0.18). These results suggested that the SKR approach is therefore able to differentiate a neutral assembly scenario from the effect of environmental filtering (stabilizing scenario) and niche differentiation (disruptive scenario) even under a high stochasticity.

SKR parameters simulated along an environmental gradient

Changing environmental conditions across communities affected local mean trait value for all the studied scenarios except the neutral one (Fig. S3). Furthermore, the variance was constant and low for the stabilizing scenario while all moments varied under the disruptive scenario (Fig. S3). For the disruptive scenario, increasing the environmental constraint (by changing the *Env* parameter from 0 to -2 or from 0 to +2) reduced the variance and increased the skewness and the kurtosis (Fig. S3a). Nevertheless, the SKR parameters calculated across communities along the gradient, and particularly the Y-intercept, consistently produced similar patterns than those observed under a fixed environment with significant differences among scenarios (Y-intercept Mo = 0.005 with low dispersal limitation, Y-intercept Mo = 0.04 with high dispersal limitation Fig. 5b). The R^2 of the SKRs also differed among scenarios with the stabilizing scenario showing the lowest range of R^2 and the disruptive scenario showing the highest R^2 (Fig. 5b).

DISCUSSION

Commonalities in trait distributions across multiple communities unveil assembly rules

Our reference neutral scenario generated a wide range of trait diversity patterns, following the view that "*simple stochastic models can reproduce natural diversity patterns*" (Hubbell 2005).

Likewise, deterministic assembly scenarios generated a wide range of trait distributions (Enquist *et al.* 2015; Le Bagousse-Pinguet *et al.* 2017). The ambiguity among scenarios further increased in our simulations as stochasticity increased or when the environmental conditions changed (e.g., sampling performed along environmental gradients). Therefore, our study therefore demonstrates that distinguishing deterministic from purely neutral patterns based on standard trait-based metrics, or by the four moments of trait distributions taken separately, is particularly challenging.

The SKR framework provided far less ambiguous insights into underlying assembly processes, as contrasting assembly scenarios exhibited distinct SKR patterns. The SKR approach did not only well discriminate the neutral from trait-based filtering scenarios, but also clearly differentiated each of the filtering scenarios from one another, irrespective of the degree of dispersal limitation, environmental condition or the size of the species pool. The SKR approach appears therefore as a promising tool to unveil assembly processes from trait distributions, even under high stochasticity, a yet important limitation of existing approaches aiming at interpreting trait diversity patterns of real-world communities (Weiher *et al.* 2011; Münkemüller *et al.* 2020).

The SKR framework shifts our perspective to focus on commonalities in trait distributions - rather than differences – to unveil assembly rules. For instance, the disruptive filtering generated a set of symmetric and asymmetric distributions. Under this scenario, increasing environmental constraints simultaneously reduced the variance and increased both the skewness and the kurtosis of trait distributions (Enquist *et al.* 2015; Le Bagousse-Pinguet *et al.* 2017), consistently with the environmental filtering hypothesis (Keddy 1992). However, the trait distributions all aligned along a specific SKR. The observed SKR pattern thus described a family of trait distributions, in which each single distribution represents an instance of a more general trait distribution operating at larger spatial scale (e.g., at the biome scale in Gross *et al.*

2017). All distributions within this family shared a common property: trait distributions are bimodal (Fig. S5), thus reflecting the effect of niche differentiation processes promoting the coexistence of functionally contrasting species (Maire *et al.* 2012). In other words, even if different environmental conditions along a gradient (and stochastic processes) can affect the shape parameters of distributions by increasing the skewness and the kurtosis separately, a bimodality persists as the signature of niche differentiation. By characterizing commonalities in trait distributions, the SKR represents a critical step toward the identification of general rules governing the functional organization of species assemblages.

By identifying families of trait distributions, the SKR framework scales up trait distributions from the community to broader geographical scales (e.g. landscape / regional / continental / biome scales). The SKR framework differs from other trait-based approaches aiming at addressing biogeographical questions by aggregating trait patterns across spatial scales (Violle *et al.* 2014; Carmona *et al.* 2016). While the SKR framework scales up trait distributions from local to wider geographical scales, it also keeps the information on the shape of trait distributions observed at the community scale. In other words, the SKR framework increases the spatial extent by quantifying trait distributions at large spatial scale but does not reduce the grain size. Therefore, the SKR framework represents an opportunity to merge community ecology and biogeography and to "*achieve a deeper understanding of biodiversity and its change across communities*" (Chase *et al.* 2018).

The skewness and the kurtosis of trait distributions are increasingly used to detect the short term effects of global change on communities, and may be used as a signal of compositional changes (Enquist *et al.* 2017; Griffin-Nolan *et al.* 2019; Wieczynski *et al.* 2019; Zhang *et al.* 2019; Aguirre-Gutiérrez *et al.* 2020). Yet, variations in skewness and kurtosis are often considered independently, i.e. without accounting for their mathematical dependency (Box 1). Observing a decrease in trait evenness (higher kurtosis) may entirely rely on changes

in the degree of skewness. Accounting for the SKR when assessing the impact of global change on ecological communities should provide additional insights on how the ecological reassembly under environmental change, and may provide a more robust validation of theoretical predictions (e.g. the "Trait Driver Theory": Enquist et al. 2015, 2017). Focusing on the distance to the lower boundary of the SKR (see Box 1) (Liu *et al.* 2020) or the deviation of individual communities from empirical to random SKR (Gross *et al.* 2017) – rather than raw variations in kurtosis - may help diagnosing shifts in community evenness and community disassembly under ongoing environmental change.

Linking theoretical predictions to empirical patterns of trait diversity

Our simulations suggest that niche differentiation and dispersal limitation jointly shape the trait diversity in real-world communities. Combining the disruptive scenario with high dispersal limitation was the only case that generated a strong family of trait distributions (i.e., a SKR with a $R^2 > 0.90$). This family of trait distributions exhibited lower kurtosis than under the neutral scenario, a pattern similar to the empirical SKRs observed in drylands worldwide (Gross et al. 2017). When simulating along an environmental gradient, the disruptive scenario also reproduced the impact of environmental filtering by reducing variance and increasing the kurtosis within communities (Fig. S3), and the shift in dominance of contrasting functional groups (e.g. the shrub-to-grass shift in dominance commonly observed in drylands; Fig. S4, Bestelmeyer *et al.* 2018). Altogether, our results corroborate the view that dryland communities are shaped by a combination of these multiple drivers.

The modelling platform *ecolottery* provides a simple and flexible environment to simulate the effect of multiple stochastic and deterministic processes on trait distributions (Munoz *et al.* 2018). Further implementations are needed to provide reliable and quantitative

predictions when comparing theoretical predictions with observed trait distributions in real-world communities:

First, different assembly processes have been shown to act differently on traits describing contrasted axes of functional specialization (e.g. size vs. resource use related-traits, Kraft *et al.* 2008; Cornwell & Ackerly 2009; Maire *et al.* 2012). On the one hand, the disruptive scenario may well apply to resource-use traits as contrasting strategies for resources acquisition and utilization may favor species coexistence (Maire *et al.* 2012). On the other hand, the directional scenario could constitute a valuable hypothesis for size-related traits in light limited environments where asymmetric competition predominates (Schamp *et al.* 2007; Gross *et al.* 2009). Considering the effect of multiple assembly processes acting on independent functional dimensions would allow a more realistic representation of community assembly and species coexistence (Maire *et al.* 2012).

Second, the distributions of trait values at large spatial scale (e.g. at the scale of the regional species pool) are important drivers determining local assembly processes and trait diversity (Carmona *et al.* 2016; Le Provost *et al.* 2017; Spasojevic *et al.* 2018). To evaluate how regional trait pools influence SKR patterns, we conducted a sensitivity analysis using different trait distributions at the regional scale (see Fig. S5 for details). Our results show that the regional trait pool influenced the SKR parameters for each scenario. It supports the need to account for the regional trait pool to provide reliable predictions on trait diversity within and across communities (Carmona *et al.* 2016; Spasojevic *et al.* 2018). Nevertheless, we also observed that the relative differences among contrasting assembly scenarios remained consistent despite variation in the composition of the regional trait pool, highlighting the robustness of the SKR approach.

Third, downscaling from a global / regional trait pool to the local community scale may require the development of a spatially-explicit framework, as contrasting assembly processes

may act simultaneously but at different spatial scale (Keddy 1992; Spasojevic *et al.* 2014; Le Provost *et al.* 2017). Such framework would allow evaluating how environmental filtering acting at broad spatial scale (Kraft *et al.* 2015; Le Bagousse-Pinguet *et al.* 2017) interacts with local biotic processes (Maire *et al.* 2012), e.g. by simulating the stabilizing and disruptive scenarios within a single framework but acting at contrasted spatial scale. In this context, further implementations of the model would allow for a more explicit representation of biotic interactions. For instance, the disruptive scenario considers a selection of two optima due to alternative suitable strategies (e.g., coexisting guilds, Cornwell & Ackerly 2009; Maire *et al.* 2012). However, the disruptive scenario does not account for interactions among individual species trough density-dependent mechanisms (MacArthur & Levins 1967) as well as for other types of biotic interactions (e.g., facilitation and indirect interactions) that have been shown to impact trait diversity in plant communities (Gross *et al.* 2009; Saiz *et al.* 2019).

Conclusions

Here we show that the skewness-kurtosis relationship (SKR) offers a powerful mean to evaluate the effect of multiple stochastic and deterministic processes on the assembly of ecological communities. By focusing on the co-variation between the skewness and the kurtosis across multiple communities, the SKR framework identifies commonalities in the shape of the trait distributions that can serve as a basis to infer assembly processes. The SKR framework is robust to stochastic processes such as variation in regional species and trait pools, dispersal limitation. Finally, our simulations suggest that the joint effect of local-scale processes such as niche differentiation and regional-scale dispersal limitation can have key implications for shaping biodiversity. Our study offers promising avenue for identifying ecological assembly rules in real-world ecosystems.

Acknowledgments

We thank the editor Brian Enquist and the three anonymous reviewers whose comments/suggestions helped improve and clarify this manuscript; Miguel Berdugo, Lucas Deschamps, Fernando T. Maestre, Pascal Monestiez and Caroline Tucker for fruitful discussions. YLB-P was supported by a Marie Sklodowska-Curie Actions Individual Fellowship (MSCA-IF) within the European Program Horizon 2020 (DRYFUN Project 656035). PL received funding from the Czech Science Foundation (GACR 17-19376S) and the Czech Academy of Sciences (RVO 67985939). CV was supported by the European Research Council (ERC) Starting Grant Project 'ecophysiological and biophysical constraints on domestication in crop plants' (grant ERC-StG-2014-639706-CONSTRAINTS). This study was partly supported by the French Foundation for Research on Biodiversity (FRB; <www.fondationbiodiversite.fr>) and EDF in the context of the CESAB project 'causes and consequences of functional rarity from local to global scales' (FREE). N.G. was supported by the AgreenSkills+ fellowship programme which has received funding from the EU's Seventh Framework Programme under grant agreement N° FP7-609398 (AgreenSkills+ contract).

REFERENCES

Aguirre-Gutiérrez, J., Malhi, Y., Lewis, S.L., Fauset, S., Adu-Bredu, S., Affum-Baffoe, K., *et al.* (2020). Long-term droughts may drive drier tropical forests towards increased functional, taxonomic and phylogenetic homogeneity. *Nature communications*, 11, 1–10.

Bestelmeyer, B.T., Peters, D.P.C., Archer, S.R., Browning, D.M., Okin, G.S., Schooley, R.L., *et al.* (2018). The Grassland–Shrubland Regime Shift in the Southwestern United States: Misconceptions and Their Implications for Management. *BioScience*, 68, 678–690.

Carmona, C.P., de Bello, F., Mason, N.W.H. & Lepš, J. (2016). Traits Without Borders: Integrating Functional Diversity Across Scales. *Trends in Ecology & Evolution*, 31, 382–394.

Chase, J.M., McGill, B.J., McGlinn, D.J., May, F., Blowes, S.A., Xiao, X., *et al.* (2018). Embracing scale-dependence to achieve a deeper understanding of biodiversity and its change across communities. *Ecology Letters*, 21, 1737–1751.

Cornwell, W.K. & Ackerly, D.D. (2009). Community assembly and shifts in plant trait distributions across an environmental gradient in coastal California. *Ecological Monographs*, 79, 109–126.

Cristelli, M., Zaccaria, A. & Pietronero, L. (2012). Universal relation between skewness and kurtosis in complex dynamics. *Phys. Rev. E*, 85, 066108.

Cullen, A.C., Frey, H.C. & Frey, C.H. (1999). *Probabilistic techniques in exposure assessment: a handbook for dealing with variability and uncertainty in models and inputs*. Springer Science & Business Media.

Denelle, P., Violle, C. & Munoz, F. (2019). Distinguishing the signatures of local environmental filtering and regional trait range limits in the study of trait–environment relationships. *Oikos*, 128, 960–971.

Diamond, J.M. (1975). The island dilemma: lessons of modern biogeographic studies for the design of natural reserves. *Biological conservation*, 7, 129–146.

Enquist, B.J., Bentley, L.P., Shenkin, A., Maitner, B., Savage, V., Michaletz, S., *et al.* (2017). Assessing trait-based scaling theory in tropical forests spanning a broad temperature gradient. *Global Ecology and Biogeography*, 26, 1357–1373.

Enquist, B.J., Norberg, J., Bonser, S.P., Violle, C., Webb, C.T., Henderson, A., *et al.* (2015). Chapter Nine - Scaling from Traits to Ecosystems: Developing a General Trait Driver Theory via Integrating Trait-Based and Metabolic Scaling Theories. In: *Advances in*

Ecological Research, Trait-Based Ecology - From Structure to Function (eds. Pawar, S., Woodward, G. & Dell, A.I.). Academic Press, pp. 249–318.

Etienne, R.S. & Alonso, D. (2005). A dispersal-limited sampling theory for species and alleles: A dispersal-limited sampling theory. *Ecology Letters*, 8, 1147–1156.

Götzenberger, L., de Bello, F., Br\aathen, K.A., Davison, J., Dubuis, A., Guisan, A., *et al.* (2012). Ecological assembly rules in plant communities—approaches, patterns and prospects. *Biological reviews*, 87, 111–127.

Griffin-Nolan, R.J., Blumenthal, D.M., Collins, S.L., Farkas, T.E., Hoffman, A.M., Mueller, K.E., *et al.* (2019). Shifts in plant functional composition following long-term drought in grasslands. *Journal of Ecology*, 107, 2133–2148.

Grime, J.P. (2006). Trait convergence and trait divergence in herbaceous plant communities: mechanisms and consequences. *Journal of Vegetation Science*, 17, 255–260.

Gross, N., Kunstler, G., Liancourt, P., Bello, F.D., Suding, K.N. & Lavorel, S. (2009). Linking individual response to biotic interactions with community structure: a trait-based framework. *Functional Ecology*, 23, 1167–1178.

Gross, N., Le Bagousse-Pinguet, Y., Liancourt, P., Berdugo, M., Gotelli, N.J. & Maestre, F.T. (2017). Functional trait diversity maximizes ecosystem multifunctionality. *Nature ecology & evolution*, 1, 0132.

Hubbell, S.P. (2001). *The Unified Neutral Theory of Biodiversity and Biogeography (MPB-32)*. Princeton University Press.

Hubbell, S.P. (2005). Neutral theory in community ecology and the hypothesis of functional equivalence. *Functional ecology*, 19, 166–172.

Keddy, P.A. (1992). Assembly and response rules: two goals for predictive community ecology. *Journal of vegetation science*, 3, 157–164.

Kraft, N.J., Adler, P.B., Godoy, O., James, E.C., Fuller, S. & Levine, J.M. (2015). Community assembly, coexistence and the environmental filtering metaphor. *Functional ecology*, 29, 592–599.

Kraft, N.J.B., Valencia, R. & Ackerly, D.D. (2008). Functional Traits and Niche-Based Tree Community Assembly in an Amazonian Forest. *Science*, 322, 580–582.

Laliberté, E. & Legendre, P. (2010). A distance-based framework for measuring functional diversity from multiple traits. *Ecology*, 91, 299–305.

Le Bagousse-Pinguet, Y., Gross, N., Maestre, F.T., Maire, V., de Bello, F., Fonseca, C.R., *et al.* (2017). Testing the environmental filtering concept in global drylands. *Journal of Ecology*, 105, 1058–1069.

Le Provost, G., Gross, N., Börger, L., Deraison, H., Roncoroni, M. & Badenhausser, I. (2017). Trait-matching and mass effect determine the functional response of herbivore communities to land-use intensification. *Funct Ecol*, 31, 1600–1611.

Leibold, M.A., Holyoak, M., Mouquet, N., Amarasekare, P., Chase, J.M., Hoopes, M.F., *et al.* (2004). The metacommunity concept: a framework for multi-scale community ecology: The metacommunity concept. *Ecology Letters*, 7, 601–613.

Liu, C., Li, Y., Zhang, J., Baird, A.S. & He, N. (2020). Optimal Community Assembly Related to Leaf Economic-Hydraulic-Anatomical Traits. *Frontiers in plant science*, 11, 341.

Loranger, J., Munoz, F., Shipley, B. & Violle, C. (2018). What makes trait-abundance relationships when both environmental filtering and stochastic neutral dynamics are at play? *Oikos*, 127, 1735–1745.

MacArthur, R. & Levins, R. (1967). The limiting similarity, convergence, and divergence of coexisting species. *The american naturalist*, 101, 377–385.

Maire, V., Gross, N., Börger, L., Proulx, R., Wirth, C., Pontes, L. da S., *et al.* (2012). Habitat filtering and niche differentiation jointly explain species relative abundance within grassland communities along fertility and disturbance gradients. *New Phytologist*, 196, 497–509.

Mason, N.W.H., Mouillot, D., Lee, W.G. & Wilson, J.B. (2005). Functional richness, functional evenness and functional divergence: the primary components of functional diversity. *Oikos*, 111, 112–118.

Mayfield, M.M. & Levine, J.M. (2010). Opposing effects of competitive exclusion on the phylogenetic structure of communities. *Ecology letters*, 13, 1085–1093.

McGill, B.J., Enquist, B.J., Weiher, E. & Westoby, M. (2006). Rebuilding community ecology from functional traits. *Trends in ecology & evolution*, 21, 178–185.

Münkemüller, T., Gallien, L., Pollock, L.J., Barros, C., Carboni, M., Chalmandrier, L., *et al.* (2020). Dos and don'ts when inferring assembly rules from diversity patterns. *Global Ecology and Biogeography*.

Munoz, F., Grenié, M., Denelle, P., Taudière, A., Laroche, F., Tucker, C., *et al.* (2018). ecolottery: Simulating and assessing community assembly with environmental filtering and neutral dynamics in R. *Methods in Ecology and Evolution*, 9, 693–703.

Munoz, F. & Huneman, P. (2016). From the Neutral Theory to a Comprehensive and Multiscale Theory of Ecological Equivalence. *The Quarterly Review of Biology*, 91, 321–342.

Ricklefs, R.E. (1987). Community diversity: relative roles of local and regional processes. *Science*, 235, 167–171.

Ridout, M.S. & Linkie, M. (2009). Estimating overlap of daily activity patterns from camera trap data. *JABES*, 14, 322–337.

Rolhauser, A.G. & Pucheta, E. (2017). Directional, stabilizing, and disruptive trait selection as alternative mechanisms for plant community assembly. *Ecology*, 98, 668–677.

Saiz, H., Le Bagousse-Pinguet, Y., Gross, N. & Maestre, F.T. (2019). Intransitivity increases plant functional diversity by limiting dominance in drylands worldwide. *Journal of Ecology*, 107, 240–252.

Schamp, B.S., Chau, J. & Aarssen, L.W. (2007). Dispersion of traits related to competitive ability in an old-field plant community. *J Ecology*, 0, 071119203335008-???

Shmida, A. & Ellner, S. (1984). Coexistence of plant species with similar niches. *Vegetatio*, 58, 29–55.

Spasojevic, M.J., Catano, C.P., LaManna, J.A. & Myers, J.A. (2018). Integrating species traits into species pools. *Ecology*, 99, 1265–1276.

Spasojevic, M.J., Copeland, S. & Suding, K.N. (2014). Using functional diversity patterns to explore metacommunity dynamics: a framework for understanding local and regional influences on community structure. *Ecography*, 37, 939–949.

Violle, C., Enquist, B.J., McGill, B.J., Jiang, L.I.N., Albert, C.H., Hulshof, C., *et al.* (2012). The return of the variance: intraspecific variability in community ecology. *Trends in ecology & evolution*, 27, 244–252.

Violle, C., Reich, P.B., Pacala, S.W., Enquist, B.J. & Kattge, J. (2014). The emergence and promise of functional biogeography. *PNAS*, 111, 13690–13696.

Weiher, E., Freund, D., Bunton, T., Stefanski, A., Lee, T. & Bentivenga, S. (2011). Advances, challenges and a developing synthesis of ecological community assembly theory. *Philosophical Transactions of the Royal Society B: Biological Sciences*, 366, 2403–2413.

Weiher, E. & Keddy, P. (2001). *Ecological assembly rules: perspectives, advances, retreats*. Cambridge University Press.

Wieczynski, D.J., Boyle, B., Buzzard, V., Duran, S.M., Henderson, A.N., Hulshof, C.M., *et al.* (2019). Climate shapes and shifts functional biodiversity in forests worldwide. *Proceedings of the National Academy of Sciences*, 116, 587–592.

Zhang, D., Peng, Y., Li, F., Yang, G., Wang, J., Yu, J., *et al.* (2019). Trait identity and functional diversity co-drive response of ecosystem productivity to nitrogen enrichment. *Journal of Ecology*, 107, 2402–2414.

SUPPORTING INFORMATION

Additional Supporting Information may be downloaded via the online version of this article at Wiley Online Library (www.ecologyletters.com).

As a service to our authors and readers, this journal provides supporting information supplied by the authors. Such materials are peer-reviewed and may be re-organized for online delivery, but are not copy-edited or typeset. Technical support issues arising from supporting information (other than missing files) should be addressed to the authors.

BOX 1: The Skewness-Kurtosis Relationship (SKR)

We examined whether the relationship between the skewness and the kurtosis of trait distributions (Fig. 1a) can help deciphering the signatures of contrasting assembly processes. The approach is inspired by optimization procedures increasingly used in physics, climatology and economy (e.g. Cristelli *et al.* 2012). We apply the approach to diagnose assembly rules from trait distributions (the Skewness-Kurtosis Relationship [SKR] approach). While the mean and variance reflect the location and the scale of a distribution (the latter being the dispersion of trait values within a community), the skewness and kurtosis inform on its shape. The degree of skewness quantifies the asymmetry of a given distribution. For instance, a skew distribution indicates the dominance of extreme trait values (see exponential distribution in Fig. 1b), which can typically arise from asymmetric competition for light (Schamp *et al.* 2007). The kurtosis quantifies the relative peakiness of a trait distribution and the relative density of its tails. Low kurtosis values reflect an even distribution of trait values within a given community, a definition of a high trait diversity (Gross et al. 2017). Low Kurtosis may reflect the coexistence of functionally contrasting species (see uniform and bimodal distributions in Fig. 1b) (Enquist *et al.* 2017; Gross *et al.* 2017). In contrast, peaked distributions characterized by high kurtosis value reflect a low trait diversity, and may typically occur under strong environmental filtering (sensu Keddy 1992) selecting for a limited range of trait value (see hyperbolic distribution in Fig. 1b).

Skewness (S) and kurtosis (K) are related through the following inequality (Fig. 1b):

$$K \geq \beta S^2 + \alpha \qquad (1)$$

This inequality generates a mathematically constrained triangle in which all possible trait distributions can be represented and characterized (Gross *et al.* 2017), i.e. the skewness-kurtosis space. For instance, the normal distribution is defined by a unique combination of skewness and kurtosis values of 0 and 3 respectively. It can therefore be represented as a single coordinate

in the skewness-kurtosis space (red dot, in Fig. 1d). Families of trait distributions can also be represented by a skewness-kurtosis relationship (SKR, hereafter) with a slope β and a Y-intercept α. A SKR implies that when trait distributions become more skewed, they also become more peaked, resulting in a decrease in evenness. The slope β of the SKR measures the strength of the relationship, i.e., the extent to which evenness decreases as trait distributions become more skewed. The Y-intercept α indicates the lowest kurtosis value at skewness = 0, and corresponds to the highest trait diversity predicted by a given SKR. Distributions belonging to a family of distributions share common properties. For instance, in the case of a skew-bimodal distribution (Fig. 1c, green dashed line in Fig. 1d), all distributions are bimodal although their degree of skewness and kurtosis can vary across communities. This would be the case when two distinct functional groups coexist within communities (e.g. grass and shrub species) but their relative abundance can vary across communities.

The inequality (1) has a lower boundary that sets a limit to the minimal kurtosis value predicted for any degree of skewness, i.e. the potential maximum trait diversity for a given skewness (black dash line, $K = S^2 + 1$, Fig. 1b) (see Gross et al. 2017 for a mathematical demonstration). The distance to the lower boundary for a given distribution - exemplified with the black arrow in the case of the exponential distribution (Fig. 1b) - thus quantifies the extent to which trait diversity departs from the potential maximum trait diversity independently from the degree of skewness. Although skewness and kurtosis individually provide valuable information on community trait distributions, the SKR approach helps to diagnose complex trait distributions (Cullen & Frey 1999) and to reveal the extent to which trait diversity is maximized within communities. Applying the SKR framework to ecological communities may allow identifying assembly rules through the identification of commonalities in the shape of the trait distributions observed across multiple communities.

Figures Legend:

Figure 1 Characterizing complex trait distributions using the Skewness-Kurtosis Relationship (SKR). (**a)** A trait distribution is a density function representing the relative frequency or abundance of trait values within a community. Examples of trait distributions include normal (panel a), uniform, bimodal, hyperbolic or exponential distributions (panel b). (c) Example of a family of distributions: a skew-bimodal distribution (see results, and Box 1). (d) The Skewness-Kurtosis space. Trait distributions are characterized by distinct skewness (S) - kurtosis (K) coordinates. Families of trait distributions can be characterized by a specific Skewness-Kurtosis Relationship (SKR) such as $K = \beta S^2 + \alpha$. The distance to the lower boundary (i.e. potential minimum kurtosis value) of a given distribution (exemplified with the black arrow in the case of the exponential distribution) quantifies the extent to which trait evenness is maximized.

Figure 2 The four moments of the trait distributions simulated under the four theoretical scenarios (Neutral [Neu], Stabilizing [Sta], Disruptive [Dis], Directional [Dir]) under **(a)** fixed environment and varying species pools, **(b)** changing environment and fixed species pool, and under low / high dispersal limitation. We represent the mean, variance, skewness and kurtosis of the trait distributions simulated under each scenario using violin plots. For each panel, we provide the mean overlap (Mo) among the four moments of the trait distributions. Different letters indicate significant differences between scenarios (overlap < 0.05; NS for Not-Significant).

Figure 3 Species richness (Sp. Rich.) and commonly-used trait diversity indices (FDis, Rao, FEve) simulated under the four theoretical scenarios (Neutral [Neu], Stabilizing [Sta], Disruptive [Dis], Directional [Dir]) in **(a)** Fixed environment varying species pools, **(b)**

changing environment fixed species pool, and under low / high dispersal limitation. We represent each predicted parameter using violin plots. For each panel, we provide the mean overlap (Mo) between the four-parameter distributions. Different letters indicate significant differences between scenarios (overlap < 0.05; but NS for Not-Significant).

Figure 4 Effect of the different assembly scenarios on the Skewness-Kurtosis Relationship (SKR) in a fixed environment and varying regional species pool. (**a)** Coordinates of the simulated communities in the skewness-kurtosis space under the different scenarios. We simulate 100 communities (number of run = 500) assembled in a constant environment under low / high dispersal limitation. Dark and light blue dots represent poor and rich regional pools, respectively. (**b)** We represent the parameters of the SKRs (R^2, Y-intercept (alpha), slope of the SKRs (beta), distance to the lower boundary) for each scenario using violin plots. We provide the mean overlap (Mo) among the four scenarios. Different letters indicate significant differences between scenarios (overlap < 0.05; but NS for Not-Significant).

Figure 5 Effect of the different assembly scenarios on the Skewness-Kurtosis Relationship (SKR) along an environmental gradient. (**a)** Coordinates of the simulated communities in the skewness-kurtosis space under the different scenarios. We simulated 100 communities (number of run = 500) assembled along an environmental gradient (from Env = -2 to Env = +2) and a fixed regional species pool (n = 150 species) under low / high dispersal limitation. Dark and light blue dots represent the environmental gradient ranging from -2 to +2. (**b)** We represent the parameters of the SKRs (R^2, Y-intercept (alpha), slope of the SKRs (beta), distance to the lower boundary) for each scenario using violin plots. We provide the mean overlap (Mo) among the four scenarios. Different letters indicate significant differences between scenarios (overlap < 0.05; but NS for Not-Significant).

FIGURES

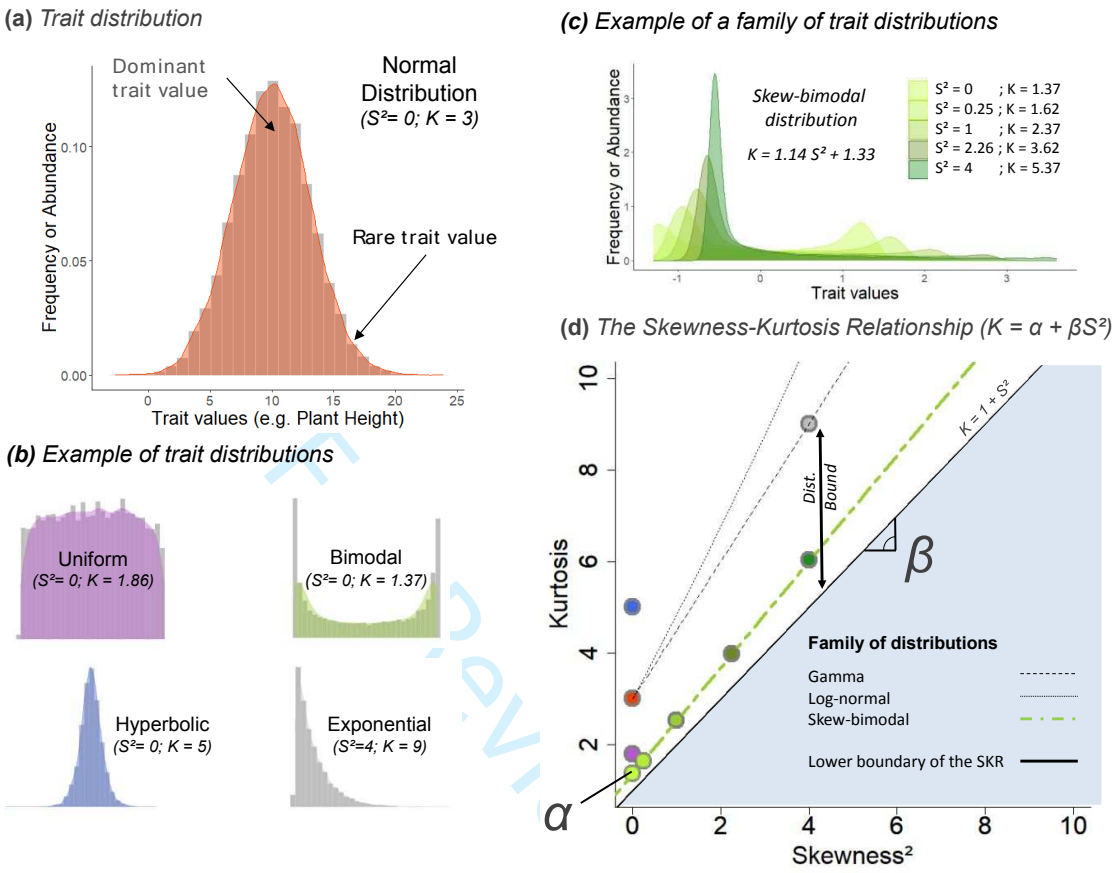

Figure 1

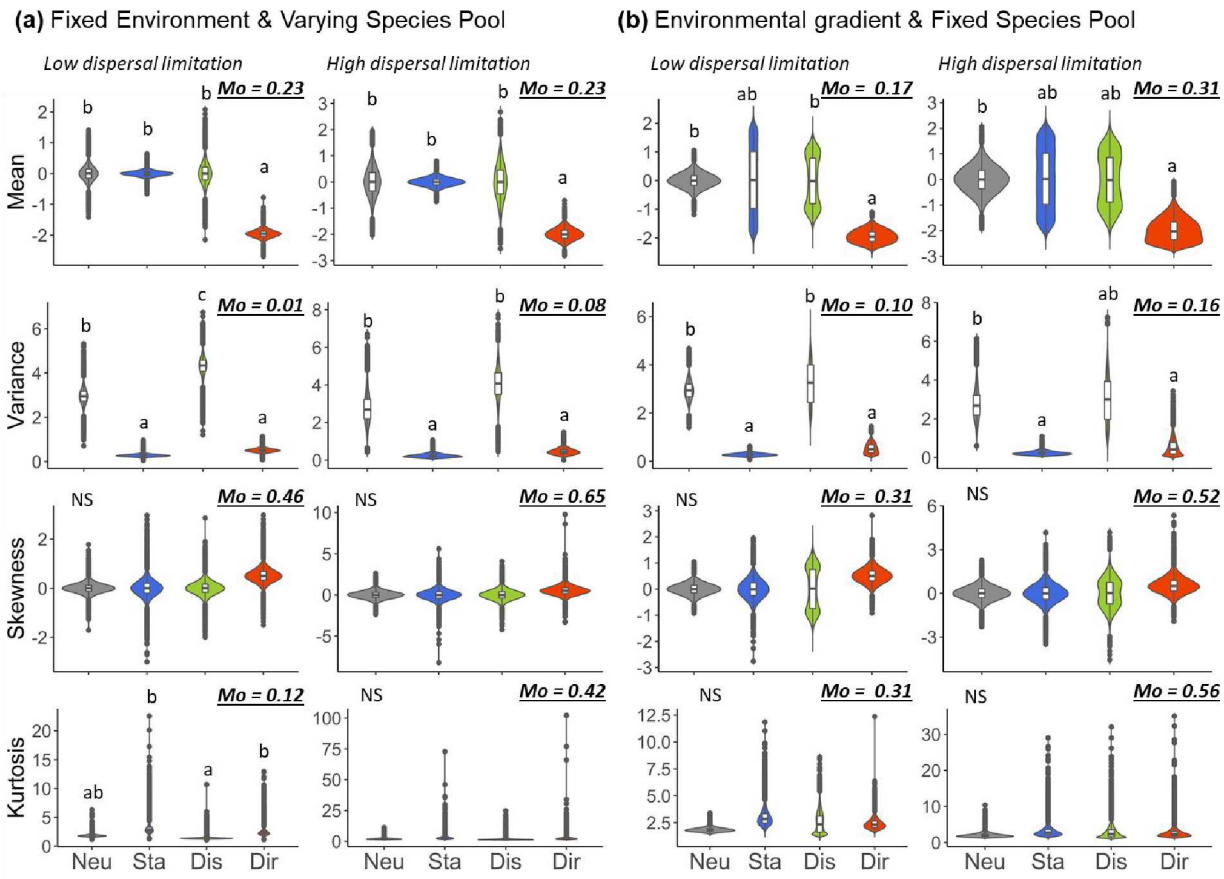
(a) Fixed Environment & Varying Species Pool
(b) Environmental gradient & Fixed Species Pool
Low dispersal limitation
High dispersal limitation
Low dispersal limitation
High dispersal limitation
Mean
Variance
Skewness
Kurtosis
Mo = 0.23
Mo = 0.23
Mo = 0.17
Mo = 0.31
Mo = 0.01
Mo = 0.08
Mo = 0.10
Mo = 0.16
Mo = 0.46
Mo = 0.65
Mo = 0.31
Mo = 0.52
Mo = 0.12
Mo = 0.42
Mo = 0.31
Mo = 0.56
NS
Neu
Sta
Dis
Dir

Figure 2

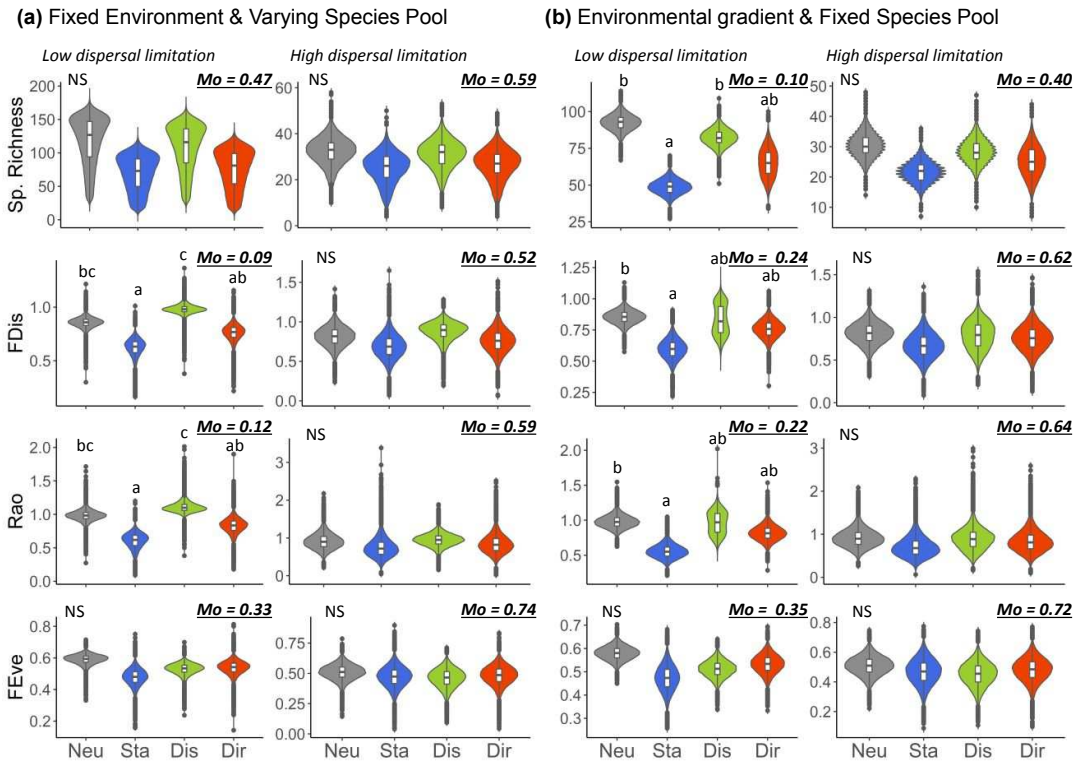

Figure 3

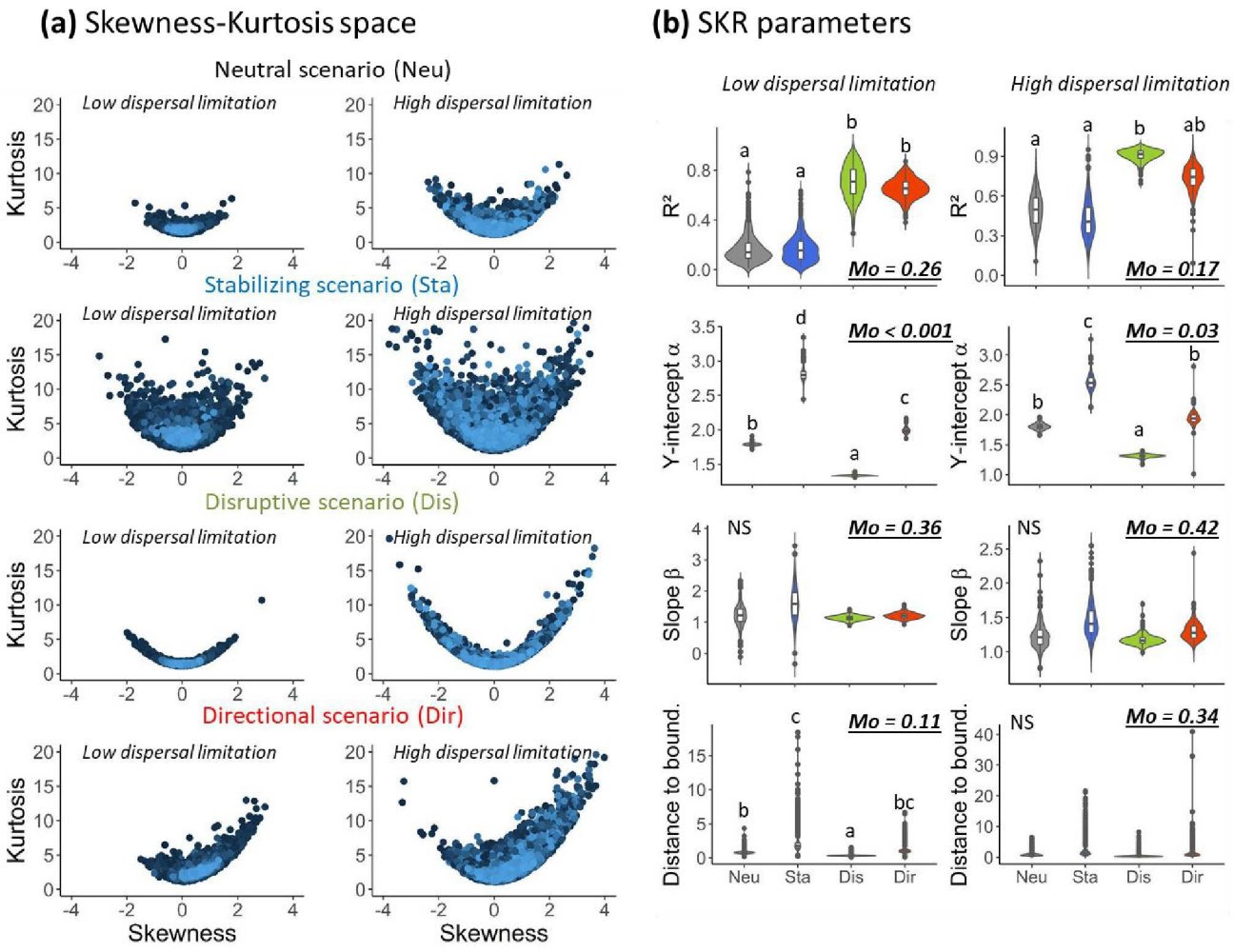
(a) Skewness-Kurtosis space
Neutral scenario (Neu)
Low dispersal limitation
High dispersal limitation
Kurtosis
Stabilizing scenario (Sta)
Disruptive scenario (Dis)
Directional scenario (Dir)
Skewness
(b) SKR parameters
R²
Mo = 0.26
Mo = 0.17
Y-intercept α
Mo < 0.001
Mo = 0.03
Slope β
NS
Mo = 0.36
Mo = 0.42
Distance to bound.
Mo = 0.11
Mo = 0.34
Neu
Sta
Dis
Dir

Figure 4

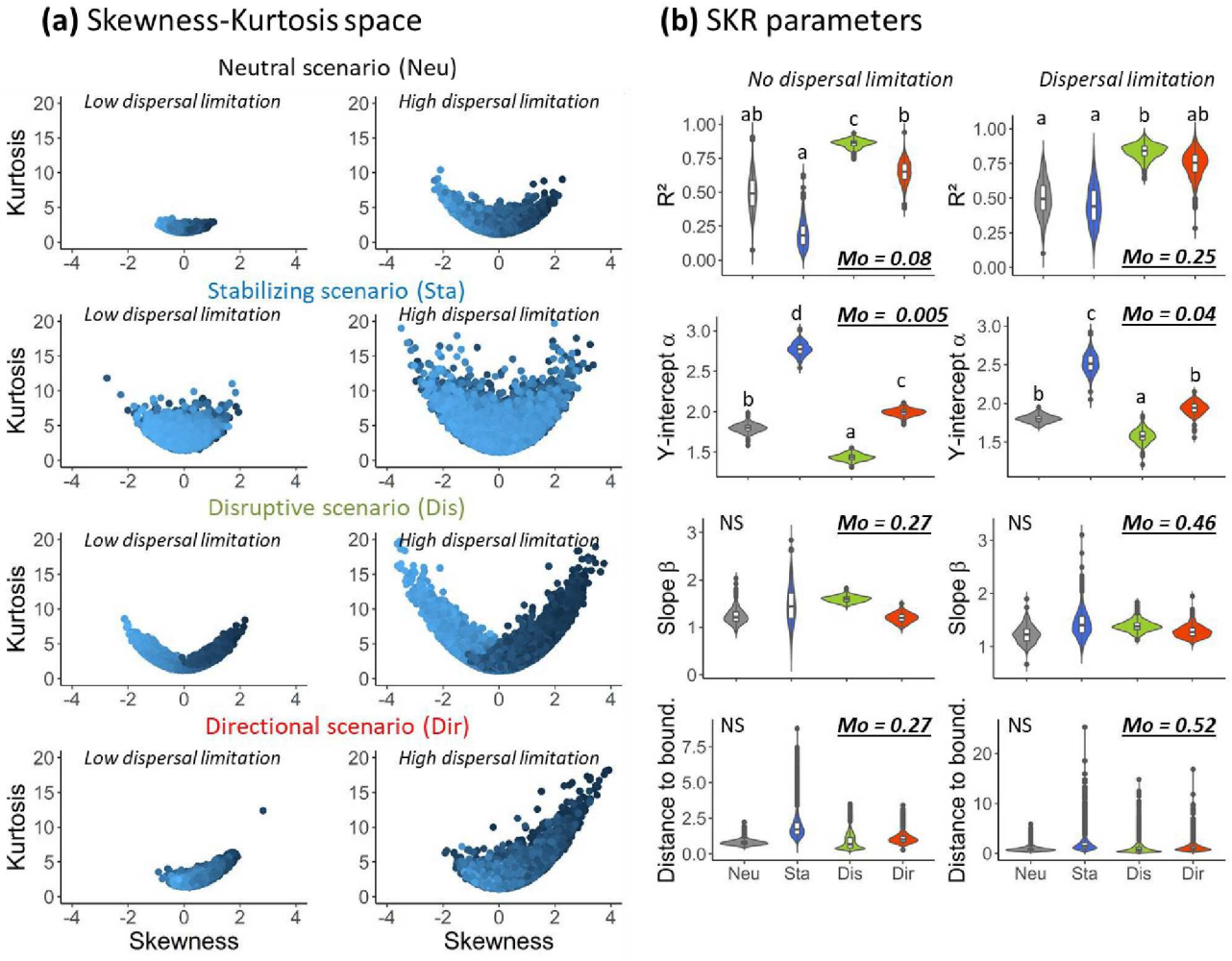
(a) Skewness-Kurtosis space
Neutral scenario (Neu)
Low dispersal limitation
High dispersal limitation
Kurtosis
Stabilizing scenario (Sta)
Disruptive scenario (Dis)
Directional scenario (Dir)
Skewness
(b) SKR parameters
No dispersal limitation
Dispersal limitation
R²
Mo = 0.08
Mo = 0.25
Y-intercept α
Mo = 0.005
Mo = 0.04
Slope β
NS
Mo = 0.27
Mo = 0.46
Distance to bound.
Mo = 0.27
Mo = 0.52
Neu
Sta
Dis
Dir

Figure 5